Available online at www.sciencedirect.com
SCIENCE DIRECT®

Journal of the European Ceramic Society 23 (2003) 2297–2306
www.elsevier.com/locate/jeurceramsoc

Modelling linear and nonlinear behavior of polycrystalline ferroelectric ceramics

Johannes Rödel*, Wolfgang S. Kreher

Institut für Werkstoffwissenschaft, Technische Universität Dresden, Hallwachsstrasse 3, 01062 Dresden, Germany

Received 6 July 2002; received in revised form 10 January 2003; accepted 24 January 2003

Abstract

A micro-electromechanical model is presented, which describes the macroscopic behavior of ferroelectric ceramics under weak signal and unipolar large signal loading conditions. The approach is based on a laminar domain structure and a hierarchical homogenization procedure, which considers grains as spherical inclusions within a homogenized effective medium. The model predicts the extrinsic effects of mobile domain walls, hysteresis at large fields, and ferroelectric fatigue by unipolar cycling. Additionally, internal fields can be estimated. As an example, numerical results and available experimental data for barium titanate ceramics are discussed.

Keywords: Effective properties; Ferroelectric properties; Micro-mechanics; Modelling

1. Introduction

Piezoelectric ceramics have attracted much attention during the last years due to the use of such materials for electromechanical actuators, transducers and other applications. Piezoelectric ceramics are always ferroelectric since it is necessary to induce a preferred orientation of polarization in a polycrystal with random crystal orientations in order to obtain macroscopic piezoelectric behavior. This so-called poling process is a result of microstructural changes caused by applied electric fields. Among piezoelectric ceramic materials, lead zirconate titanate (PZT) is especially attractive because of its high piezoelectric coefficients. Barium titanate is another example from the same class of materials with perovskite structure which show ferroelectric and ferroelastic behavior.

The microstructure of ferroelectric materials is characterized by domain patterns. They exhibit often laminar or 3-dimensionally banded structures within a single crystallite.[1] Macroscopic electrical and mechanical response is strongly affected by the domain structure and its changes under applied electric field or stress. Domains contribute to the linear macroscopic dielectric, piezoelectric and elastic constants by reversible domain wall motions even under very small fields.[2,3] At higher fields, irreversible domain wall motions as well as nucleation and growth of domains with new orientations cause very strong nonlinear effects (e.g. the so-called butterfly curves) and hysteresis.

The technological importance and scientific complexity of the nonlinear electromechanical behavior has stimulated many different attempts to model the electromechanically coupled constitutive behavior of ferroelectric ceramics. Phenomenological models describe the material response on the basis of thermodynamic relations and make use of internal variables in order to take into account hysteresis effects. Different types of models have been developed.[4–7] They are constructed directly on the macro-level and suitable for calculations of macroscopically inhomogeneous fields. Although the internal variables and their evolution laws can be motivated by microscopic considerations, the phenomenological models cannot give more insight into the physics of the microstructural process.

Thus, recent reviews[8,9] have pointed out the need of microelectromechanical models to explain and describe quantitatively the correlation between microstructure,

* Corresponding author. Tel.: +49-351-46331414; fax: +49-351-46331422.
E-mail address: roedel@tmfs.mpgfk.tu-dresden.de (J. Rödel).

0955-2219/03/$ - see front matter © 2003 Elsevier Ltd. All rights reserved.
doi:10.1016/S0955-2219(03)00084-0

domain wall motions and macroscopic response of ferroelectric materials. Micro-electromechanical models can be classified into linear and nonlinear models. There are several investigations concerning the calculation of effective linear properties of piezoelectric polycrystals.[10–16] Some of these neglect the domain structure[10,13,14]) but especially Turik et al.[11,12,15] and Aleshin[16] took into account ferroelectric domain structures. They have revealed the importance of ferroelectric domains also in this regard.

Concerning nonlinear material behavior most of the published models disregard the domain structure of the crystallites and consider switching of the grain orientation according to different switching laws.[17–22] They differ in the way how the grain interaction is taken into account. For instance Hwang et al.[17] have neglected the grain interactions. They have developed an energetic criterion for switching and have been able to calculate large signal hysteresis curves. Huber et al.[23] have published a ferroelectric extension of a classical model of polycrystal plasticity describing the nonlinear behavior of ferroelectric ceramics. In this approach, the grains consist of domains with all possible orientations and different volume fractions. The volume fractions of the domains are determined by a dissipative law. As in most of the models which consider grain interactions,[18–20] an effective medium is assumed into which spherical grains are embedded. An alternative approach considering grain interactions is the calculation by finite element models.[21,22]

Besides load dependence, ferroelectrics often show remarkable time dependent effects like aging, deaging and fatigue, which limits the reliability of ferroelectric materials. In the context of this paper, we understand fatigue as a degradation of ferroelectric properties with increasing number of (electrical or mechanical) load cycles and distinguish it from time dependent degradation under constant load (aging) or load dependent damage like cracking or dielectric breakdown.

The primary indication of fatigue is the decrease of remnant polarization (and often increase of coercive field) in bipolar cycling experiments.[24] Fatigue is also accompanied by decreasing dielectric and piezoelectric constants of the polycrystals.[25] In the case of unipolar cycling, which is more important for actuator applications, fatigue is much less distinct but also leads to decrease of the polarization change and strain change per cycle.[26] Despite extensive studies, a generally accepted explanation of ferroelectric degradation and fatigue is still lacking. The pinning of domain walls by different types of defects has often been considered as the main ferroelectric fatigue mechanism (for an overview see Ref. 24). To the knowledge of the authors, fatigue models have not yet been included into micro-mechanical constitutive models of ferroelectrics.

The aim of the present work is to develop a micro-electromechanical model which is able to describe effective linear properties of ferroelectric ceramics as well as their large signal behavior and fatigue effects. The model is designed to cover the conditions under service of ferroelectric actuators which are usually subjected to unipolar electric fields. Under these conditions the switching of the domain orientations is not the dominating process. Instead, the domain structure, generated by the poling process, changes only gradually.

The paper is organized as follows: the next section gives a brief overview of the applied model, including the basic equations, a multi-domain effective medium approach, nonlinearity due to domain wall motion and a ferroelectric fatigue process. Then some numerical results, concerning remnant and effective properties, internal fields and nonlinear behavior, are shown. First examples of modeling the degradation of ferroelectric properties during unipolar cycling are presented as well. Finally the results are discussed and compared with measured data.

2. Model

2.1. Basic equations

The mechanical and electrical field quantities considered in a piezoelectric solid are the stress $\sigma_{ij}(\mathbf{x})$, the strain $\gamma_{ij}(\mathbf{x})$, the dielectric displacement $D_i(\mathbf{x})$ and the electric field $E_i(\mathbf{x})$. $\mathbf{x}$ is the position vector. The electric field vector is defined by the gradient of the electric potential Φ, and the strain is defined by the displacement u_i assuming linear theory with small displacements

$$E_i(\mathbf{x}) = -\frac{\partial}{\partial x_i}\Phi(\mathbf{x}), \quad \gamma_{ij}(\mathbf{x}) = \frac{1}{2}\left[\frac{\partial}{\partial x_j}u_i(\mathbf{x}) + \frac{\partial}{\partial x_i}u_j(\mathbf{x})\right] \tag{1}$$

When no body forces and free charges are present, the fields have to satisfy the equilibrium equations

$$\frac{\partial}{\partial x_j}\sigma_{ij}(\mathbf{x}) = 0, \quad \frac{\partial}{\partial x_i}D_i(\mathbf{x}) = 0 \tag{2}$$

On the surface of the body we have appropriate boundary conditions according to prescribed electric fields and prescribed stress.

Assuming linear response of the material, the field quantities are related by the linear piezoelectric constitutive equations

$$\begin{aligned}\gamma_{ij} &= s^E_{ijkl}\sigma_{kl} + d_{kij}E_k + \gamma^s_{ij}\\ D_i &= d_{ikl}\sigma_{kl} + \varepsilon^\sigma_{ik}E_k + P^s_i\end{aligned} \tag{3}$$

or in an abbreviated vector-matrix notation, obtained if the usual Voigt tensor indices replacement is utilized:

$$\boldsymbol{\gamma} = \mathbf{s}^E\boldsymbol{\sigma} + \mathbf{d}^t\mathbf{E} + \boldsymbol{\gamma}^s$$
$$\mathbf{D} = \mathbf{d}\boldsymbol{\sigma} + \varepsilon^\sigma\mathbf{E} + \mathbf{P}^s \quad (4)$$

Here s_{ijkl} is the elastic compliance tensor, ε_{ik} is the dielectric permittivity, and d_{ijk} is the piezoelectric coupling tensor. γ^s_{ij} denotes the spontaneous (stress free) strain in a short-circuited solid (vanishing stress and electric field) due to the ferroelectric/ferroelastic phase transformation. P^s_i is the spontaneous polarization. In this work the macroscopic response is considered at room temperature only, and a non-polarized stress-free state (corresponding to cubic symmetry) serves as a reference state.

Due to random orientation of grains in polycrystals the material properties in ceramics depend on spatial position x, and the field quantities $\boldsymbol{\sigma}(\mathbf{x})$, $\boldsymbol{\gamma}(\mathbf{x})$, $\mathbf{E}(\mathbf{x})$ and $\mathbf{D}(\mathbf{x})$ become random functions, which are locally related by the constitutive Eq. (3) or (4). Considering homogeneous applied electrical and mechanical fields, the statistical expectation values of the fluctuating internal fields are constant and equal to the macroscopically applied fields:

$$\langle\boldsymbol{\gamma}(\mathbf{x})\rangle = \bar{\boldsymbol{\gamma}} \quad \langle\boldsymbol{\sigma}(\mathbf{x})\rangle = \bar{\boldsymbol{\sigma}}$$
$$\langle\mathbf{D}(\mathbf{x})\rangle = \bar{\mathbf{D}} \quad \langle\mathbf{E}(\mathbf{x})\rangle = \bar{\mathbf{E}} \quad (5)$$

The angular brackets denote an appropriate statistical averaging operation.

It is the objective of the model to relate the macroscopic values of strain and dielectric displacement as well as the internal field quantities to the prescribed stress and electric field. In general the macroscopic fields are related by a set of constitutive equations similar to (4):

$$\bar{\boldsymbol{\gamma}} = \mathbf{s}^{E*}\bar{\boldsymbol{\sigma}} - \mathbf{d}^{t*}\bar{\mathbf{E}} + \boldsymbol{\gamma}^{s*}$$
$$\bar{\mathbf{D}} = \mathbf{d}^*\bar{\boldsymbol{\varepsilon}} + \boldsymbol{\varepsilon}^{\sigma*}\mathbf{E} + \mathbf{P}^{s*}. \quad (6)$$

In the linear case the effective material properties (denoted by an asterisk) are constants which have to be calculated dependent on the microstructural properties. Note that the effective remnant constants $\boldsymbol{\gamma}^{s*}$ and $\mathbf{P}^{s*}$ are not simple averages of the local properties since the grain material constants and the grain remnant properties are correlated.

For non-linear material behavior, the effective and the remnant properties become dependent on the applied fields $\bar{\boldsymbol{\sigma}}$ and $\bar{\mathbf{E}}$. In general this dependency must be described by an incremental relationship as will be discussed below.

2.2. Multi-domain effective medium approach

In order to calculate the effective material properties we apply a multi-scale homogenization procedure. First, homogenized crystallite properties are calculated using a particular domain model and, second, the effective polycrystal properties are calculated using an effective medium approach (Fig. 1). In this paper we assume a simple domain structure following the work of Arlt.[27] The grains consist of 90 °C domains which are arranged in a laminar stack. Then the average grain behavior can be described by homogenized properties which relate the average grain stress and polarization to the average strain and electric field of the crystallite in a form analogous to (4). The homogenized properties depend on the microscopic single-crystal properties $\mathbf{s}^E$; $\mathbf{d}$, $\boldsymbol{\varepsilon}^\sigma$, $\boldsymbol{\gamma}^s$ and $\mathbf{P}^s$, and on the volume fractions of the two types of domains. The derivation of the explicit relations by standard laminate theory (neglecting small perturbations at the grain boundary) is straightforward and will not be given here.

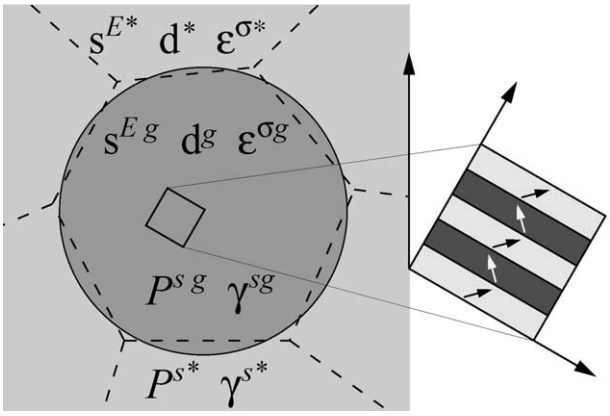

Fig. 1. Micro-mechanical model: inclusion with laminar domain structure embedded in a homogeneous effective medium. The individual domains possess single-crystal properties, whereas homogenized grain properties are denoted by a superscript g.

The calculation of the effective polycrystal properties according to Eqs. (5) and (6) requires the knowledge of average fields in the crystallites. In order to calculate these fields we consider the individual grains of the polycrystal to be spherical inclusions, characterized by the locally homogenized crystallite properties and surrounded by an infinite homogeneous medium having the effective macroscopic properties. This represents the elementary piezoelectric inclusion problem which is solved e.g. by Dunn and Wienecke[28] making use of the so-called Eshelby tensor of a piezoelectric solid. This procedure leads to the well known effective medium approximation (EMA, sometimes also called self-consistent scheme), which considers the interaction of the crystallites in a statistically averaged manner.

An improved description of ferroelectric materials must take into account the domain wall motion under higher external fields. If the driving force on a domain wall is sufficiently high to move it, the local material properties (linear crystallite properties including spontaneous strain and polarization) will change. The effective material behavior is therefore nonlinear. In this situation the constitutive law Eq. (6) is of no use, because the effective properties become non-unique

functions of the applied fields. Instead it must be incrementally linearized. When we rewrite (6) in a condensed notation as

$$\bar{\mathbf{j}} = \mathbf{L}^*\bar{\mathbf{f}} + \mathbf{j}^{s*}, \tag{7}$$

where $\bar{\mathbf{j}}$ is a vector formed from the relevant strain and electric displacement tensor components and $\bar{\mathbf{f}}$ represents stress and electric field, its differential form reads:

$$\mathrm{d}\mathbf{j} = \mathrm{d}\mathbf{L}^*\bar{\mathbf{f}} + \mathbf{L}^*\mathrm{d}\mathbf{f} + \mathrm{d}\mathbf{j}^{s*}. \tag{8}$$

This means that the change of the macroscopic strain and dielectric displacement is a result of the changes of effective linear properties and the changes of the remnant strain and polarization, which are dependent on the absolute level of the applied fields according to an incremental load history. The changes d**L*** and d$\mathbf{j}^{s*}$ for a given load step are obtained in a straightforward manner from current internal fields and the effective linear properties of the previous incremental load step.

The model so far considers only the linear part of the interaction of crystallites what leads to somewhat over-estimated constraints. This approximation of linear constraints even in the range of macroscopic nonlinear material behavior has been developed by Kröner[29] for a similar model of polycrystal plasticity. It has been shown that this approximation gives reasonable results.

2.3. Domain wall motion

In order to take into account the effect of changing local domain configurations, a criterion for the domain wall motion has to be applied. In the present model that criterion will be based on the potential energy difference associated with a change of domain volume fractions.[30,31] The potential energy (under prescribed stresses and electric fields it is equivalent to the free enthalpy) of the system becomes a function of the microstructural state and the applied fields.

We use here the volume fraction of one domain type as the local internal state variable ξ. The volume fraction of the other domain type is $1-\xi$. Domain wall motion changes the volume fractions and causes changes of the effective crystallite properties (e.g. polarization). Note that ξ completely characterizes the present state of the system and is not only the change of the system. Additionally, we assume that any change of the volume fraction of domains by domain wall displacement is associated with energy dissipation. We define the dissipated energy by

$$W_D = \int_0^{\xi_{\mathrm{acc}}} D(\xi_{\mathrm{acc}})\ \mathrm{d}\xi_{\mathrm{acc}} \tag{9}$$

where ξ_{acc} is the accumulated change of ξ

$$\xi_{\mathrm{acc}} = \int_{\xi_0}^{\xi} |\mathrm{d}\xi|.$$

$D(\xi_{\mathrm{acc}})$ is a characteristic material function, and ξ_0 characterizes the initial state of the system. The dissipation function $D(\xi_{\mathrm{acc}})$ is equivalent to the critical thermodynamic driving force necessary to move the domain wall.

For quasi-static processes we can assume in every load step that the release of potential energy is completely consumed by the domain wall dissipation

$$\Delta\dot{U}_p(\xi) + \dot{W}_D(\xi) = 0. \tag{10}$$

This equation relates the thermodynamic driving force to the rate of energy dissipation and determines an equilibrium domain configuration.

2.4. Ferroelectric fatigue

It has been shown, that ferroelectric fatigue is connected with local polarization switching.[26] From a phenomenological point of view the pinning of domain walls corresponds to an increase of the critical driving force. Therefore, we can couple the increase of the critical driving force with the domain wall motion, which is given by the accumulated change of the volume fraction ξ_{acc}. In this paper we postulate a dissipation function of the following form:

$$D = D_0 + D_{\mathrm{act}}[1 - \exp(-p\ \xi_{\mathrm{acc}})] \tag{11}$$

where D_0 is an initial or threshold value according to the critical driving force in an unfatigued crystal and D_{act} can be interpreted as a contribution due to activation of defects. The defect activation takes place with the activation rate parameter p and depends on the accumulated change of the domain volume fraction.

3. Results

3.1. Experimental data input

Numerical simulations using the presented model require a set of microscopic information. First of all, microscopic (single-domain single crystal) properties are necessary to calculate the macroscopic behavior of ceramics. Single-crystal properties are not available for important materials like PZT. For this reason we have chosen $BaTiO_3$ to demonstrate the potential of the model. $BaTiO_3$ is seen as a typical ferroelectric material with tetragonal structure. It is well investigated and many properties are published. For numerical calculations we have used a single-crystal data set shown in Table 1.

The orientation distribution function (ODF) of the crystallites is another important input information. For unpoled ceramics there is no reason to doubt about a

Table 1
Properties of $BaTiO_3$ single-domain single-crystals,[32] spontaneous strains and polarization[33]

$\frac{s_{11}^E}{m^2/N}$	$\frac{s_{12}^E}{m^2/N}$	$\frac{s_{13}^E}{m^2/N}$	$\frac{s_{33}^E}{m^2/N}$	$\frac{s_{55}^E}{m^2/N}$	$\frac{s_{66}^E}{m^2/N}$
7.4×10^{-12}	-1.4×10^{-12}	-4.4×10^{-12}	13.1×10^{-12}	16.4×10^{-12}	7.6×10^{-12}
$\frac{d_{31}}{pm/V}$	$\frac{d_{33}}{pm/V}$	$\frac{d_{15}}{pm/V}$	$\frac{\varepsilon_{11}^\sigma}{As/Vm}$	$\frac{\varepsilon_{33}^\sigma}{As/Vm}$	
−33.4	90.0	540	39×10^{-9}	1.1×10^{-9}	
γ_{11}^s	γ_{33}^s	$\frac{P_3^s}{C/m^2}$			
-3.5×10^{-3}	7×10^{-3}	0.26			

random distribution. However, for poled ceramics the ODF in the bulk of the material is unknown and cannot be determined with standard experimental techniques. For that reason in this work a simple model will be employed, which does not model the poling process itself, but simply has to give a reasonable model for the anisotropy and macroscopic polarization. To this end, we start from a random orientation distribution and switch all crystallites with an angle between the crystallite polarization and the macroscopic polarization higher than $\pi-\theta_p$ by 180°. The resulting poling state is characterized by the poling angle θ_p, which can vary between 0 (unpoled state) and 0.5π (fully poled according to this model).

Further microscopic information concerning the domain wall motion is also difficult to obtain from experiments reported in the literature. In this work, values for the dissipation constant and the fatigue parameters are chosen so that the qualitative behavior of the model becomes clearly visible but not to fit the behavior of a particular material.

3.2. Remnant properties

Remnant strain and polarization of ferroelectric ceramics are a result of the poling process. Unpoled ceramics have no macroscopic polarization, yet an isotropic volume strain as compared to the cubic reference state may occur which is due to elastic interaction of the crystallites. After poling the orientation distribution function is changed which leads to a macroscopic polarization and strain change. Figs. 2 and 3 show results obtained with and without relaxation of domain fractions. Properties without relaxation are calculated with fixed volume fractions of 0.5 for each domain type. The curves with domain relaxation are obtained by the nonlinear model using $D=0$ to allow full relaxation without energy dissipation.

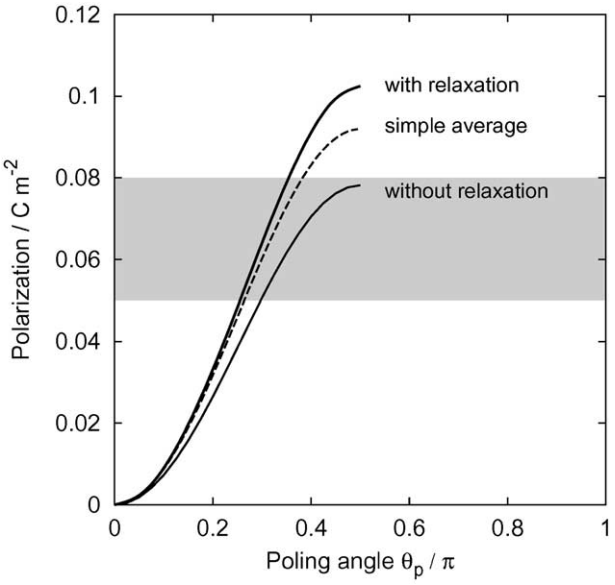

Fig. 2. Remnant polarization of $BaTiO_3$ polycrystals with polydomain crystallites depending on the poling state. Poling states are characterized by an orientation distribution function, described in the text, with a poling angle θ_p. The gray band indicates the typical range of experimental values.

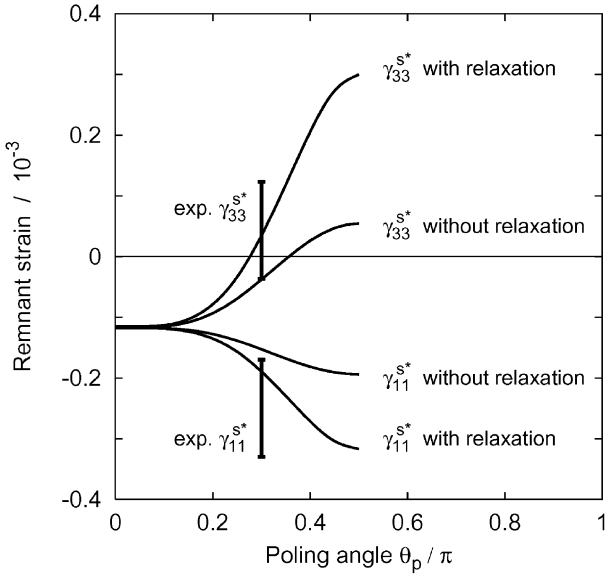

Fig. 3. Calculated and measured remnant strains for $BaTiO_3$. Calculated results are shown depending on the poling state.

Within our model the remnant properties can be calculated for different poling states, characterized by the angle θ_p. As the orientation distribution of the grains is not accessible from experiment, it is difficult to compare the calculated results with measured data. The grey band in Fig. 2 represents typical values for the remnant polarization of $BaTiO_3$ ceramics.[34] From this comparison we have chosen a polarization state characterized by $\theta_p \approx 0.3\pi$ to compare the following calculated results with measured data.

Fig. 3 shows calculated and measured remnant strains. Various measurements have been reported for the lateral strain γ_{11}^s.[33,35,36] The error bar on the corresponding data point represents these results. The lowest value for γ_{11}^s and the only accessible value for γ_{33}^s had been reported in.[33] For that reason, the error bar for the strain in poling direction is estimated from the lateral strain, taking the data from[33] as a lower bound.

3.3. Linear material properties

Effective material properties of ferroelectric ceramics are a result of a superposition of intrinsic and extrinsic contributions. In our model both parts can be calculated. Effective intrinsic properties are obtained using the linear effective medium approach with mixed volume fractions of domains (e.g. $\xi = 0.5$). Extrinsic contributions are a result of reversible domain wall motions. Here effective material properties are calculated by applying electric fields up to 1 kV/mm parallel and perpendicular to the poling direction and with the dissipation constant set to $D = 0$. This allows again a relaxation of the domain volume fractions without energy dissipation and the calculations include intrinsic and extrinsic contributions.

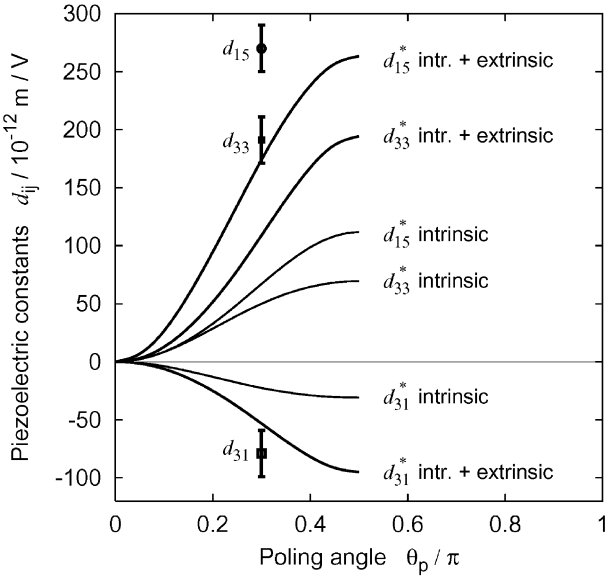

Fig. 4. Piezoelectric constants dependent on the polarization angle. The curves show results for fixed domain walls (intrinsic constants, thin lines) and results for moving domain walls (intrinsic and extrinsic contributions, thick lines). The data points depict a typical set of measured values.

Table 2
Calculated and measured dielectric constants of $BaTiO_3$ ceramics

	$\varepsilon_{11}^\sigma/\varepsilon_0$	$\varepsilon_{33}^\sigma/\varepsilon_0$
Measured	1620	1900
Calculated	2300	2300

The resulting strain and dielectric displacement curves turned out to be almost linear. The effective piezoelectric constants d_{ij} in Fig. 4 are calculated from the slope of the curves and plotted depending on the poling state. For comparison, the calculated intrinsic piezo-constants are shown. The calculated results are compared with experimental data.[33] The error bars are estimated, representing typical results for $BaTiO_3$.

The calculated effective dielectric constants (Table 2) depend only slightly on the poling state of the material. Additionally, they are almost isotropic. The calculated values of ε_{11}^σ and ε_{33}^σ vary between 19.8–21.9×10^{-9} As/Vm and 19.6–21.8×10^{-9} As/Vm, respectively.

3.4. Unipolar hysteresis behavior

We consider now the dissipative motion of domain walls. Under large electric fields one observes a hysteretic material behavior. Fig. 5 shows the dielectric displacement under unipolar electric fields as a typical result of numerical simulation. The simulation is performed for a fully poled state ($\theta_p = 0.5\pi$) and has been started with equal domain volume fraction ($\xi = 0.5$) for each crystal orientation. The structure was allowed to relax completely during the first ten steps under $\bar{E} = 0$ causing an initial polarization of 0.1025 C = m^2. This procedure changes the somewhat artificial initial state into an equilibrium state within the constraints of our model.

From the first increment of the external electric field the domain wall motion is associated with energy dissipation according to the described model. In the example the parameters are set to $D_0 = 100$ kJ/m^3, $D_{act} = 100$ kJ/m^3 and $p = 10$. As a result, the domain walls do not move until the driving force exceeds a critical value. The curve is initially linear with a slope

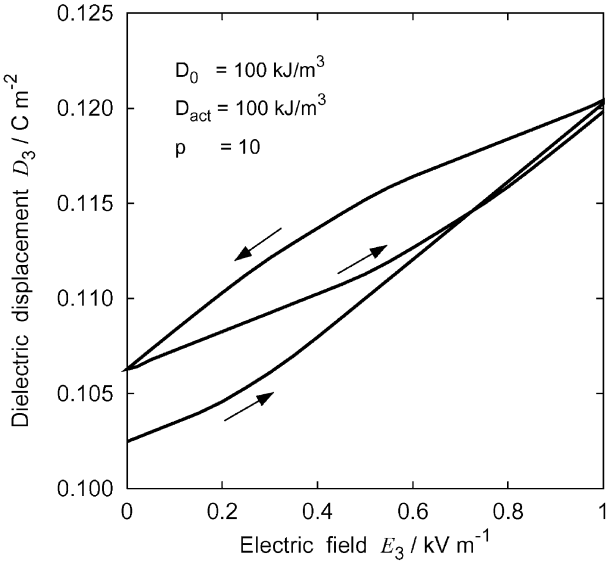

Fig. 5. Calculated unipolar hysteresis curve.

which corresponds to the effective intrinsic dielectric constant. With increasing field some domain walls start to move and the slope of the curve increases. After sufficient decrease of the electric field below the maximum ($\bar{E} = 1$ kV/mm), the stored energy provides the driving force to move domain walls backwards while the driving force due to externally applied fields decreases with the applied field.

The curve shows a hysteretic behavior as it is expected from unipolar experiments. The macroscopic hysteresis curve can be characterized by the area of the loop, which corresponds to the energy loss or dissipated energy per cycle, and by the average slope of the loop, which can be interpreted as the effective large signal dielectric constant.

3.5. Ferroelectric fatigue behavior

Repeated loading and unloading of a ferroelectric material in the large signal regime may cause a deterioration of ferroelectric properties. This ferroelectric fatigue behavior can be simulated using our history dependent approach for the dissipation. As a result, hysteresis behavior (dissipated energy per cycle, maximum polarization change and actuation strain as well as average slope of the loop) becomes dependent upon the number of loading cycles. Figs. 6 and 7 show typical predictions of this model for the dissipated energy per cycle and the average slope of the loop. Curves are drawn for different values of the defect activation rate, which are set to rather high values in order to obtain clear effects within a limited number of calculations. But the qualitative behavior is independent of particular values of the defect activation rate. The latter parameter only scales the characteristic process along the number of cycles. The results show that after a small number of cycles the characteristic quantities decrease with ln N but later they approach a saturation value, as it is expected from experiments.

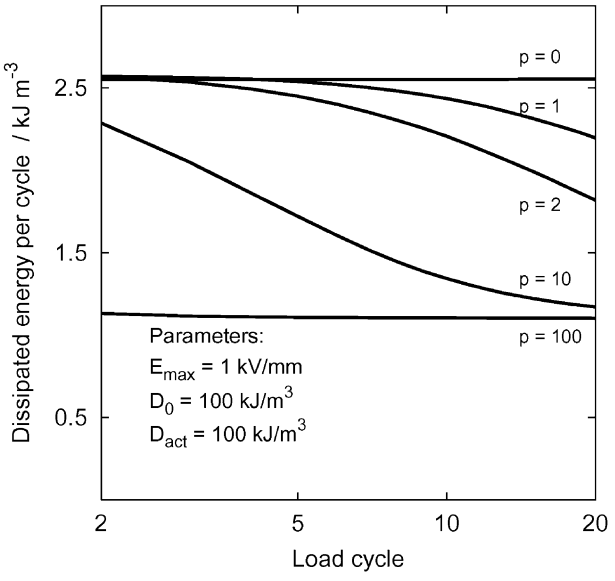

Fig. 6. Dissipated energy per unipolar cycle.

3.6. Internal fields

As the presented approach for the macroscopic behavior is based on a microscopic model, it is not only able to describe the effective behavior. Additionally it is also capable of making some statements concerning internal fields. The knowledge of internal fields is important to understand further effects like damage by microcracks.

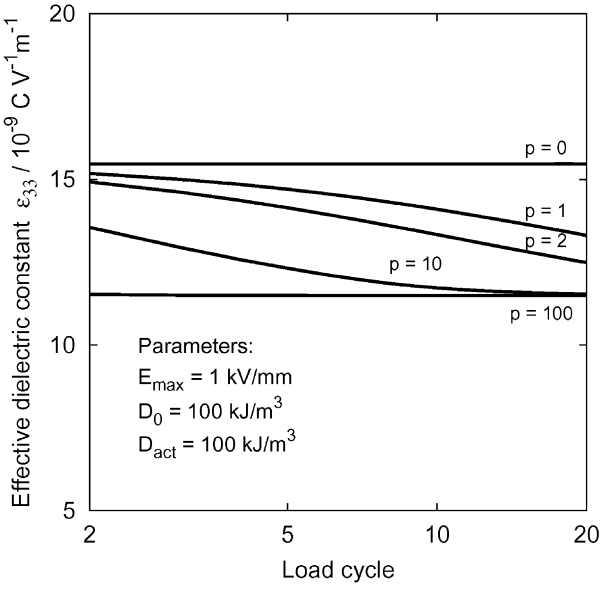

Fig. 7. Effective large signal dielectric constant.

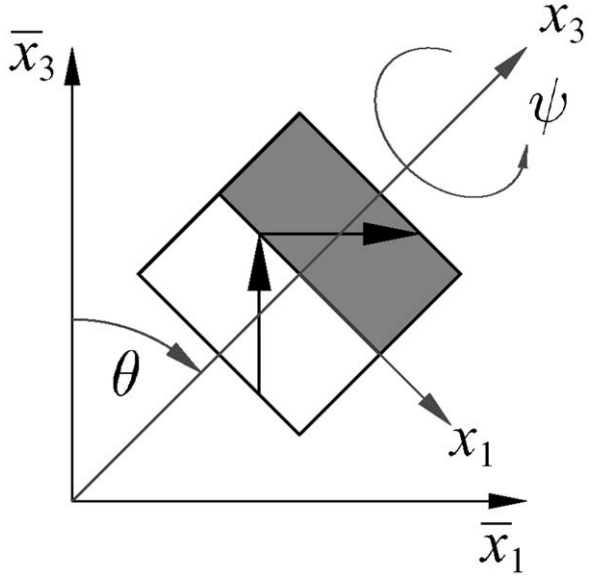

Fig. 8. Crystallite orientation and relationship between local (crystal) and global (sample) coordinate systems.

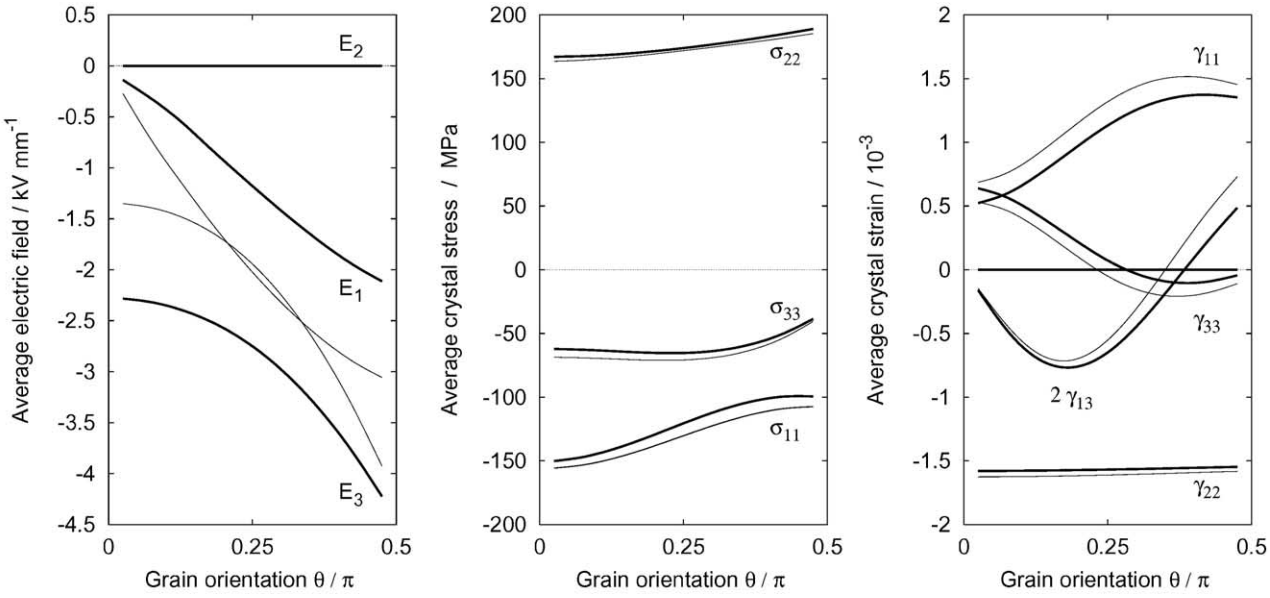

Fig. 9. Internal electric fields, stresses and strains in local (crystallite) coordinates. The field quantities express the mean values within a poly-domain grain depending on the grain orientation θ and for fixed orientation angle $\psi = 0$. Thick lines represent the field values under zero external electric field and thin lines represent a state under 1 kV/mm parallel to the sample 3-axis.

Fig. 9 shows internal electric fields, stresses and strains. The fields are calculated in a local coordinate system (see Fig. 8) and are dependent on the grain orientation θ ($\psi = 0$). The calculations are again performed for the highest poling state ($\theta_p = 0.5\pi$), where all angles θ are smaller than 0.5π. Additionally, the dissipation constant was set to zero to allow maximum relaxation. The field quantities express mean values within a poly-domain grain, i.e. the fields are averaged over the particular domain structure. The internal stresses and electric fields turned out to be fairly high and the influence of an externally applied field on the mechanical fields is rather small. Maximum tensile stresses occur in x_2-direction (perpendicular to the polarization vectors of both domain types).

4. Discussion

In this section we discuss the effects of some of our assumptions and simplifications on the behavior of the model. Generally it can be stated that the model describes several important properties of ferroelectric ceramics, like nonlinearity and hysteresis as well as intrinsic and extrinsic contributions to the effective properties. However, since experimental results may depend on additional conditions, like grain size, dopants, poling conditions, which we do not take into account in our model, the comparison of measured and calculated data gives more a qualitative assessment of the model. On the other hand, it should be kept in mind that the model does not contain any adjustable parameters—except the dissipation parameters. All results are strictly based on the microscopic properties.

Besides the orientation distribution function, which has been already briefly discussed in Section 3.2, the material model is determined on the microscopic scale by the assumption of a laminar domain structure. One should recognize that this domain structure is a strong idealization of the domain patterns observed in real materials.[1] The applied domain model allows an accommodation of the spontaneous strains in only two directions, whereas in real polycrystals different laminar domain stacks will be arranged in a hierarchical way to give the possibility for three-dimensional release of internal stresses. Thus, the laminar domain model may over-estimate the remnant polarization and strain (Figs. 2 and 3) as well as the resulting internal fields (Fig. 9).[1] An opposite effect may be caused by free charge carriers, which can screen crystal polarization at the grain boundaries. This effect would decrease the average polarizations but not or much less the strain. Concerning the linear material properties, the results show that the model predicts the electromechanical response in the correct order of magnitude. However, the calculated piezoelectric constants, corresponding to a poling state which fits experimental polarization, are somewhat too small. This may have different reasons. As described above, the laminar domain structure is more restricted in its possibilities to respond to external

[1] Only for fine grained ceramics (barium titanate grain size less than 5 μm), the simple two-dimensional laminar domain pattern is the more probable structure.[37] On the other hand, it is known that for fine grained ceramics the effective properties become dependent on the grain size.[38,39] Although no details about the grain size are given in the referred experimental work, it can be assumed that the data refer to coarse grained ceramics.

load by reversible domain wall motion. A better agreement could also be obtained with a higher degree of poling. This would not contradict the measured remnant polarization if one took into account charge screening at the grain boundaries and/or complex domain structures.

Furthermore one should note, that our effective medium approach is based on the linear (elastic, dielectric and piezoelectric) contributions in the interaction between the crystallites only. Nonlinear effects which would lead to a weaker interaction are not considered. On the other hand, in our model the reversible domain wall motion is constrained only by the grain interaction. Additional internal retarding forces are not considered. So the resulting over-estimation of the extrinsic contribution is expected to be compensated by the stiffer effective medium.

Besides the piezoelectric coupling constants the model gives results also for the dielectric and elastic constants. The dielectric constants are slightly higher than the experimental results, yet the extrinsic contributions are correctly predicted (see e.g. Ref. 2). The results for effective elastic properties, however, are much stiffer than the experimental values. This may be attributed to microcracks which are always present in these ceramics and which have strong effects on elastic properties.[40]

Including a history dependent dissipation function, the model can be used to simulate effects which depend on the number of loading cycles like fatigue and deaging. The functional dependence of the critical driving force on the accumulated domain wall motion reflects the fact that the domain wall pinning is caused by defects which have to be activated for instance by reorientation and rearranging. The first numerical examples show that the utilized phenomenological approach reproduces the unipolar fatigue behavior in the sense of decreasing average slope and area of the unipolar hysteresis curves.[26]

Although the simple fatigue model is a phenomenological model, it is based on microscopic considerations and should be useful to discuss the implications of microscopic fatigue models.

The model of domain wall motion assumes that the dissipation constant is dependent on the accumulated change of the domain fraction only, but not on the present driving force. Thus the model can not consider reversible and irreversible domain wall motions simultaneously. This assumption has certain consequences on the calculated large signal response. The initial slope in Fig. 5 is caused only by the intrinsic contribution and is therefore much smaller than the value expected from experiments. Additionally, the neglected nonlinear contribution in the grain interaction may affect the calculated behavior in a manner, which underestimates the large signal behavior. Therefore, future work has to modify the model in such a way, that at small driving forces, below a critical level, domain walls can move reversibly.

5. Summary and conclusion

In this paper we have presented a micro-electromechanical model of the macroscopic behavior of ferroelectric ceramics. The approach is based on a simple laminar domain structure and a hierarchical homogenization procedure. It considers the extrinsic effects of mobile domain walls, hysteresis at large fields and ferroelectric fatigue by unipolar cycling. The results show the correlation between the domain structure and several macroscopic properties. Therefore the model offers the possibility to obtain information about processes relevant on the microscale from measurements on the macroscale.

Furthermore it has been shown that a micro-electromechanical model is very attractive because it gives the complete tensorial description of macroscopic properties on the basis of microscopic crystal constants and a very small number of adjustable scalar parameters and is also appropriate to simulate hysteretic and path dependent effects. Regarding loading conditions of practical importance which do not cause complete switching of the domain orientations, the laminar domain approach with movable domain walls has turned out to be an adequate description. Besides the material behavior under electric fields, considered in this paper, the model is also capable to simulate the behavior under mechanical or combined electro-mechanical loading conditions. So it can be expected, that the described micro-electromechanical model may be successfully applied for other highly interesting electromechanical applications.

Acknowledgements

This work was supported by the Deutsche Forschungsgemeinschaft in the research program "Multifunctional ceramics". The work has benefited from helpful discussions with various participants of the DFG program, particularly H. Keßler, D. Lupascu, M. Kamlah, T. Hauke, R. Steinhausen and A. Schönecker. We thank also R. Müller for his help in numerical evaluation.

References

1. Arlt, G. and Sasko, P., Domain configuration and equilibrium size of domains in $BaTiO_3$ ceramics. *J. Appl. Phys.*, 1980, **51**, 4956–4960.
2. Arlt, G., Dederichs, H. and Herbiet, R., 90°-domain wall relaxation in tetragonally distorted ferroelectric ceramics. *Ferroelectrics*, 1987, **74**, 37–53.
3. Li, S., Cao, W. and Cross, L., The extrinsic nature of nonlinear

behavior observed in lead zirconate titanate ceramic. *J. Appl. Phys*., 1991, **69**, 7219–7224.
4. Kamlah, M. and Tsakmakis, C., Phenomenological modeling of the non-linear electro-mechanical coupling in ferroelectrics. *Int. J. Solids Struct*., 1999, **36**, 669–695.
5. Kamlah, M. and Jiang, Q., A constitutive model for ferroelectric PZT ceramics under uniaxial loading. *Smart Mater. Struct*., 1999, **8**, 441–459.
6. Huber, J. and Fleck, N. A., Multi-axial electrical switching of a ferroelectric: theory versus experiment. In *Smart Structures and Materials 2000: Active Materials Behavior and Mechanics, Vol. 3992 of Proceedings of SPIE*, ed. C. S. Lynch. SPIE, 2000, pp. 288–295.
7. Landis, C. M., Symmetric constitutive laws for polycrystalline ferroelectric ceramics. In *Smart Structures and Materials 2001: Active Materials Behavior and Mechanics, Vol. 4333 of Proceedings of SPIE*, ed. C. S. Lynch. SPIE, 2001, pp. 271–278.
8. Kamlah, M., Ferroelectric and ferroelastic piezoceramics—modeling of electromechanical hysteresis phenomena. *Cont. Mech. Thermodyn*., 2001, **13**, 219–268.
9. Hall, D. A., Nonlinearity in piezoelectric ceramics. *J. Mater. Sci*., 2001, **36**, 4575–4601.
10. Marutake, M., A calculation of physical constants of ceramic barium titanate. *J. Phys. Soc. Japan*, 1956, **11**, 807–814.
11. Bondarenko, E. I., Topolov, V. Y. and Turik, A. V., The effect of 90° domain wall displacements on piezoelectric and dielectric constants of perovskite ferroelectric ceramics. *Ferroelectrics*, 1990, **110**, 53–56.
12. Turik, A. V. and Topolov, V. Y., Ferroelectric ceramics with a large piezoelectric anisotropy. *J. Phys. D: Appl. Phys*., 1997, **30**, 1541–1549.
13. Pertsev, N. A., Zembilgotov, A. G. and Waser, R., Aggregate linear properties of ferroelectric ceramics and polycrystalline thin films: calculation by the method of effective piezoelectric medium. *J. Appl. Phys*., 1998, **84**, 1524–1529.
14. Li, J. Y., The effective electroelastic moduli of textured piezoelectric polycrystalline aggregates. *J. Mech. Phys. Solids*, 2000, **48**, 529–552.
15. Turik, A. V., Topolov, V. Y. and Aleshin, V. I., On a correlation between remanent polarization and piezoelectric coeffcients of perovskite-type ferroelectric ceramics. *J. Phys. D: Appl. Phys*., 2000, **33**, 738–743.
16. Aleshin, V. I., Properties of anisotropic piezoactive polycrystals. *J. Appl. Phys*., 2000, **88**, 3587–3591.
17. Hwang, S. C., Lynch, C. S. and McMeeking, R. M., Ferroelectric/ferroelastic interactions and polarization switching model. *Acta Metall. Mater*., 1995, **43**, 2073–2084.
18. Chen, X., Fang, D. N. and Hwang, K. C., Micromechanics simulation of ferroelectric polarization switching. *Acta Mater*., 1997, **45**, 3181–3189.
19. Chen, W. and Lynch, C. S., A micro-electro-mechanical model for polarization switching of ferroelectric materials. *Acta Mater*., 1998, **46**, 5303–5311.
20. Lu, W., Fang, D.-N. and Hwang, K.-C., Nonlinear electric-mechanical behavior and micromechanics modelling of ferroelectric domain evolution. *Acta Mater*., 1999, **47**, 2913–2926.
21. Hwang, S. C. and McMeeking, R. M., A finite element model of ferroelastic polycrystals. *Int. J. Solids Struct*., 1999, **36**, 1541–1556.
22. Hwang, S. C. and Waser, R., Study of electrical and mechanical contribution to switching in ferroelectric/ferroelastic polycrystals. *Acta Mater*., 2000, **48**, 3271–3282.
23. Huber, J. E., Fleck, N. A., Landis, C. M. and McMeeking, R. M., A constitutive model for ferroelectrics. *J. Mech. Phys. Solids*, 1999, **47**, 1663–1697.
24. Nuffer, J., Lupascu, D. C. and Rödel, J., Damage evolution in ferroelectric PZT induced by bipolar electric cycling. *Acta Mater*., 2000, **48**, 3783–3794.
25. Levstik, A., Bobnar, V., Kutnjak, Z., Filipiè, C. and Kosec, M., The correlation between fatigue and material constants of PLZT ceramics. *J. Eur. Ceram. Soc*., 1999, **19**, 1233–1236.
26. Pan, W., Yue, C.-F. and Tosyali, O., Fatigue of ferroelectric polarization and the electric field induced strain in lead lanthanum zirconate titanate ceramics. *J. Am. Ceram. Soc*., 1992, **75**, 1534–1540.
27. Arlt, G., Switching and dielectric nonlinearity of ferroelectric ceramics. *Ferroelectrics*, 1996, **189**, 91–101.
28. Dunn, M. L. and Wienecke, H. A., Inclusions and inhomogeneities in transversely isotropic piezoelectric solids. *Int. J. Solids Struct*., 1997, **34**, 3571–3582.
29. Kröner, E., Zur plastischen Verformung des Vielkristalls. *Acta Metall*., 1961, **9**, 155–161.
30. Rödel, J. and Kreher, W. S., Self-consistent modelling of nonlinear effective properties of polycrystalline ferroelectric ceramics. *Comput. Mater. Sci*., 2000, **19**, 123–132.
31. Rödel, J. and Kreher, W. S., Modeling of domain wall contribution to the effective properties of polycrystalline ferroelectric ceramics. In *Smart Structures and Materials 2000: Active Materials: Behavior and Mechanics, Vol. 3992*, ed. C. S. Lynch. SPIE, 2000, pp. 353–362.
32. Zgonik, M., Bernasconi, P., Duelli, M., Schlesser, R., Günter, P., Garrett, M. H., Rytz, D., Zhu, Y. and Wu, X., Dielectric, elastic, piezoelectric, electro-optic and elasto-optic tensors of $BaTiO_3$ crystals. *Phys. Rev*., 1994, **B50**, 5941–5949.
33. Landolt-Börnstein, *Numerical Data and Functional Relationships in Science and Technology, Vol. 16a of New Series III*. Springer Verlag, Berlin, 1980.
34. Jona, F. and Shirane, G., *Ferroelectric Crystals*. Pergamon Press, Oxford, 1962.
35. Uchida, N. and Ikeda, T., Electrostriction in perovskite-type ferroelectric ceramics. *Jpn. J. Appl. Phys*., 1967, **6**, 1079–1088.
36. Berlincourt, D. and Krueger, H. H. A., Domain processes in lead titanate zirconate and barium titanate ceramics. *J. Appl. Phys*., 1959, **30**, 1804–1810.
37. Arlt, G., Twinning in ferroelectric and ferroelastic ceramics: stress relief. *J. Mater. Sci*., 1990, **25**, 2655–2666.
38. Arlt, G., Hennings, D. and de With, G., Dielectric properties of fine-grained barium titanate ceramics. *J. Appl. Phys*., 1985, **58**, 1619–1625.
39. Randall, C. A., Kim, N., Kucera, J.-P., Cao, W. and Shrout, T., Intrinsic and extrinsic size effects in fine-grained morphotropic-phase-boundary lead zirconate titanate. *J. Am. Ceram. Soc*., 1998, **81**, 677–688.
40. Qin, Q.-H., Mai, Y.-W. and Yu, W.-W., Effective moduli for thermopiezoelectric materials with microcracks. *Int. J. Fracture*, 1998, **91**, 359–371.